

HOMOGENEOUS NUCLEATION IN SUPERSATURATED VAPORS OF n-NONANE

Vladimir ZDIMAL^a, Jiri SMOLIK^a and Ivo G. N. MEIJER^b

^a *Institute of Chemical Process Fundamentals,*

Academy of Sciences of the Czech Republic, 165 02 Prague 6-Suchbát, The Czech Republic

^b *Delft University of Technology, 2628 BL Delft, The Netherlands*

Received December 10, 1992

Accepted April 7, 1993

The upward thermal diffusion cloud chamber was used to measure the supersaturations of n-nonane vapors required to cause an observed rate of homogeneous nucleation of 1 droplet/cm³ s. New temperature-dependent correlations for the surface tension and the density of n-nonane have been applied in theoretical prediction of the corresponding supersaturation. The measurements are found to be in reasonable agreement with the predictions of the classical (Becker–Döring) theory whereas both the Dillmann–Meier and the Girshick–Chiu theories lead to a significant underestimation of supersaturation in the whole range of temperatures measured.

Several experimental techniques have been used to study nucleation in vapors (expansion and thermal diffusion cloud chambers, nozzles, molecular beams and shock tubes) and various organic compounds and water have been used in these investigations^{1,2}. Among these substances, n-nonane is widely used for testing the nucleation theories and for intercomparing the various experimental approaches^{3–6}. It was found that the low nucleation rate experiments carried out by using the thermal diffusion cloud chamber^{3,4} are close to the predictions by classical theory of homogeneous nucleation⁷ while the high nucleation rate measurements obtained by expansion cloud chambers^{5,6} are closer to the predictions of Reiss–Katz–Cohen theory⁷. Recently, several new theories of homogeneous nucleation based on the droplet model have appeared in literature^{8,9} which indicate better agreement with the diffusion cloud chamber experiments. Further, there appeared also refined data on physical properties of n-nonane necessary for the evaluation of experiments and comparison with theory¹⁰.

In our previous paper¹¹ we have developed a photographic technique which allows us to observe the real behavior of thermal diffusion cloud chamber. In this paper we report results obtained with this new technique concerning the supersaturations of n-nonane vapors required to cause an observed rate of homogeneous nucleation of 1 droplet/cm³ s in dependence on temperature. These results were then compared with the data published earlier^{3,4}, with the predictions given by the classical theory of homogeneous nucleation⁷, and with two new theories (Dillmann–Meier⁸ and Girshick–Chiu⁹) as well.

EXPERIMENTAL

Compounds

n-Nonane (Aldrich Chemie Steinheim, Germany), purity of 99%, was used without further purification. Helium (Messer Griesheim GmbH., Austria) was available in purity of 99.996%.

Apparatus

The chamber used here is almost identical with that described in previous papers^{12,13}. Therefore, only a brief review of the experimental technique is presented.

The thermal diffusion cloud chamber is an apparatus that utilizes nonisothermal diffusion of vapors to produce supersaturation. Physically, the chamber is a flat cylindrical vessel which consists of two metal disks separated by a glass ring. The bottom plate with a shallow pool of liquid is heated, vapor diffuses through an inert gas and condenses on the cooler top plate. The top plate is slightly conical, so that the condensate flows to its edge and along the glass wall back to the pool. At a steady state, the profiles of partial vapor pressure P_v and temperature T decrease from the bottom to the top almost linearly but the equilibrium vapor pressure of n-nonane P_{eq} decreases with temperature nearly exponentially. Therefore, the vapor in the chamber is supersaturated with maximum supersaturation $S = P_v/P_{eq}$ reached close to the top plate. By increasing the temperature difference between both plates, one can achieve the state when the nucleation begins with a measurable rate. To record the condensation, the chamber is illuminated with a thin vertical ribbon of laser beam and the droplets generated by homogeneous nucleation are photographed. This method makes it possible: (i) to determine the position of the nucleation zone; (ii) to measure the nucleation rate; (iii) to check whether the chamber operates at a steady state and (iv) to check whether the measurements are not influenced by phoretic effects¹¹.

The chamber used here had the distance between both the plates in the symmetry axis 23.8 mm, giving with the inner diameter of the chamber 163 mm the 7.1 : 1 diameter to height ratio (computed from the average distance between plates because of the conicity of the top plate). The temperature of each plate was measured with a NiCr-Ni thermocouple. The total pressure in the chamber was obtained by reading a mercury manometer. To reduce the condensation of the vapor on the wall, the glass cylinder was heated with 6 resistant wires wrapped around.

A part of the chamber volume was illuminated with a flattened laser beam 0.4 mm thick and high enough to mark visible traces both on the bottom and on the top of the chamber. This beam was obtained from a cylindrical laser beam (He-Ne, 5 mW, 632.8 nm) focused by the optical system consisting of one converging lens with radial symmetry and three converging cylindrical lenses – two vertical and one horizontal. A camera supplied with a 135 mm objective mounted on adjustable bellows was focused on the center of the chamber.

The typical experimental run proceeded as follows: The chamber was filled with n-nonane so that the liquid pool thickness on the bottom plate was about 0.6 mm and then it was flushed with helium several times. Then the whole apparatus was both optically (by a black light absorbing cloth) and thermally (using Styrofoam rings) insulated from the surroundings. The temperatures of both plates and the total pressure were adjusted so that the visually observed homogeneous nucleation rate was approximately 1 droplet/cm³ s. After that the system was left at rest for approximately half an hour to ensure complete equilibration. Then two or three photographs of the falling droplets were taken to check that the chamber operated in the steady state without convection and to determine the actual nucleation rate (by dividing the number of recorded droplets by the volume of the nucleation zone and the exposition time used). Finally, the stability of the nucleation rate was checked by the second

visual measurement and the conditions in the chamber (temperatures of both plates or the total pressure) were changed for a new experiment.

Data Evaluation

The evaluation of experimental data is based on the numerical solution of heat and mass transport equations for the partial vapor pressure of n-nonane and the temperature in the chamber. Assuming the plane parallel diffusion of vapors through a stagnant inert gas, these equations are usually³ written in the form:

$$\frac{dP_v}{dz} = \frac{(P_v - P_t)N_v}{T^s D_{vg}^0} + \frac{\alpha_{vg} P_v (P_v - P_t)}{TP_t} \frac{dT}{dz} \quad (1)$$

$$\frac{dT}{dz} = \lambda_{vg}^{-1} \left\{ -Q + N_v \left[\int_{T_2}^T C_{p,v} dT + \Delta H_v(T_2) + \alpha_{vg} RT \frac{(P_v - P_t)}{P_t} \right] \right\} \quad (2)$$

To obtain the profiles of temperature and partial vapor pressure and both fluxes in the chamber, these equations were solved numerically (by the method of iterative linearization¹⁴) on subjecting to the following boundary conditions:

$$\begin{aligned} z = 0 & \quad T = T_1 & \quad P_v = P_{v,eq}(T_1) \\ z = h & \quad T = T_2 & \quad P_v = P_{v,eq}(T_2) . \end{aligned} \quad (3)$$

Knowing the profiles of temperature and partial vapor pressure, the variation of the supersaturation with the axial distance in the chamber and hence with temperature can be calculated as

$$S(T) = P_v / P_{v,eq}(T) . \quad (4)$$

With respect to almost linear variation of partial vapor pressure and temperature with the axial distance in the chamber and practically exponential dependence of the equilibrium vapor pressure on temperature, the supersaturations calculated according to Eq. (4) reveal distinct peak located close to the top plate. Physical properties we used for these calculations are listed in Appendix.

RESULTS AND DISCUSSION

Since diffusion cloud chamber measurements are very sensitive to the intensity of the electric heating of the glass wall¹⁵, prior to the experiments we carried out a preliminary study to determine the adequate power input to the resistant wires wrapped around the glass cylinder. For this purpose the power input was changed in the interval of 0 – 21 W and the tracks of droplets generated by homogeneous nucleation were photo-

graphed. It was found that at lower power input (0 – 3.5 W) the droplets appearing in the middle of the chamber fell straight to the bottom of the chamber, but at higher power input the tracks of these droplets started to be slightly curved. It indicated that macroscopic convection cell setting up along the heated wall started to influence the conditions in the center of the chamber. Therefore, to eliminate the possible influence of wall heating, the power input we used in experiments presented here was 0 – 3.5 W. Simultaneously, the behavior of the droplets was checked by using the photographs, and the experiments in which slight convection was observed were not evaluated.

The supersaturations of n-nonane vapor required to cause the homogeneous nucleation rate of approximately 1 droplet/cm³ s were measured in the temperature range of 260 – 350 K and the total pressure range of 27.3 – 219.3 kPa. The maximum value of the total pressure was given by fear of rupturing the glass cylinder.

The experimental conditions at which the measured rate of homogeneous nucleation was approximately 1 droplet/cm³ s are listed in Table I. Using the data from Table I, the variation of supersaturation of n-nonane vapor with temperature for each experiment was calculated from Eqs (1) – (4). The maximum error in determination of the peak of supersaturation in individual experiments was found to be about 2.5%. Peaks of supersaturations for all experiments are plotted versus temperature in Fig. 1. They are compared with the theoretical predictions of variation of supersaturation with temperature for the same rate of nucleation on using the classical (Becker–Döring⁷), Dillmann–Meier⁸, and Girshick–Chiu⁹ nucleation theories; these predictions are also shown in

TABLE I
Experimental conditions under which homogeneous nucleation rate was approximately 1 droplet/cm³ s

Experiment No.	T_1 , K	T_2 , K	P_t , kPa
1	327.0	250.6	29.5
2	329.1	252.8	27.3
3	335.4	252.9	96.4
4	358.6	274.6	92.7
5	369.0	284.6	97.4
6	376.2	291.3	101.6
7	337.6	252.8	138.2
8	344.4	258.6	142.0
9	355.1	268.2	147.4
10	391.7	304.7	165.7
11	381.3	291.1	203.0
12	388.2	298.6	209.4
13	398.0	308.8	219.3

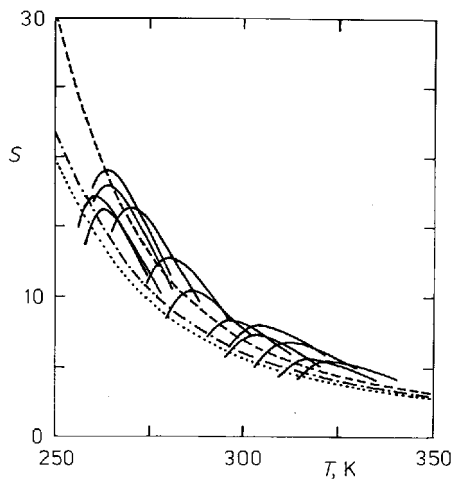


FIG. 1

Experimental supersaturations S of n-nonane vapor required for homogeneous nucleation rate of 1 droplet/cm³ s in dependence on temperature T (solid curves) – a comparison with theory : classical (---), Dillmann–Meier (·····), Girshick–Chiu (-·-·-)

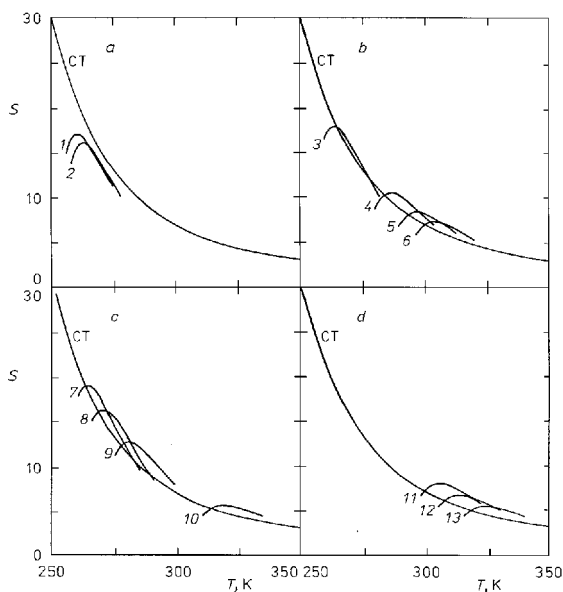


FIG. 2

Experimental supersaturations S of n-nonane vapor required for homogeneous nucleation rate of 1 droplet/cm³ s in dependence on temperature T for different total pressure (P) ranges : *a* 27.3 – 29.5 kPa, *b* 92.7 – 101.6 kPa, *c* 138.2 – 165.7 kPa, *d* 203.0 – 219.3 kPa. Numbered curves are theoretical solution (see Table I); CT – classical theory of homogeneous nucleation

Fig. 1. Physical properties necessary for the theoretical predictions are also listed in Appendix. In case of agreement of the experiment with theory, the theoretical prediction should form an envelope to the individual peaks of supersaturation. Thus, as one can see in Fig. 1, the classical theory⁷ yields better prediction than both the Dillmann–Meier⁸ and the Girshick–Chiu⁹ theories.

Further, we investigated in more details the influence of the total pressure on homogeneous nucleation in n-nonane vapor. For this purpose we arranged the experiments from Table I into four groups having near total pressure. So grouped experiments are compared with predictions by classical nucleation theory in Fig. 2a – 2d. It is apparent that the supersaturations of n-nonane, necessary to cause the same rate of nucleation, increase (for the same temperature) with the total pressure, which is in agreement with the recent findings of the other workers¹⁶.

In addition, we compared our results with the preceding published data³. The consistency of both the sets of results was surprisingly good, which confirms that our chamber was well behaved.

APPENDIX

Physical properties of both compounds were taken from the paper of Hung et al.⁴, critical constants of n-nonane from the paper of Dillmann and Meier⁸ with Pitzer acentric factor being calculated from definition equation¹⁷. For the second virial coefficient of n-nonane, the corresponding states relation proposed by Tsionopoulos¹⁸ was employed. Force constants for the Lennard–Jones (6 – 12) potential were determined from viscosity data⁴ by the method given in the book by Hirschfelder et al.¹⁹. Temperature dependences of the equilibrium vapor pressure and surface tension were taken from the paper of Viisanen and Strey¹⁰, semiempirical equation of Majer et al.²⁰ was used for enthalpy of vaporization. Thermal diffusion factors were estimated from the first Kihara approximation to the Chapman–Enskog theory¹⁹, the calculated values were correlated by the equation suggested by Kokugan and Shimizu²¹. The parameters of the dependence of mixture thermal conductivity λ_{vg} on composition A_{vg} and A_{gv} were estimated by Mason–Saxena method¹⁷.

n-Nonane

$$M = 128.257 \cdot 10^{-3} \text{ kg mol}^{-1}$$

$$T_b = 424.0 \text{ K}$$

$$T_c = 594.56 \text{ K}$$

$$P_c = 2.313 \cdot 10^6 \text{ Pa}$$

$$V_c = 5.48 \cdot 10^{-4} \text{ m}^3 \text{ mol}^{-1}$$

$$\omega = 0.444$$

$$\sigma = 6.7977 \cdot 10^{-10} \text{ m}$$

$$\varepsilon/k = 583 \text{ K}$$

$$C_p = 100.654 + 0.0475985T + 1.54483 \cdot 10^{-3}T^2 - 1.526068 \cdot 10^{-6}T^3$$

$$\lambda_g = -1.167598 \cdot 10^{-2} + 7.47947 \cdot 10^{-5}T$$

$$\lambda_l = 2.27038 \cdot 10^{-1} - \dots - 4T$$

$$\eta_g = 5.8805 \cdot 10^{-7}T^{1.5}/(T + 305.09)$$

$$\log \eta_l = -4.88174 + 510.67/T$$

$$\rho_l = 733.503 - 0.787562(T - 273.15) - 9.68937 \cdot 10^{-5}(T - 273.15)^2 - 1.29616 \cdot 10^{-6}(T - 273.15)^3$$

$$\gamma = 24.7316 - 0.099236(T - 273.15) + 8.38083 \cdot 10^{-5}(T - 273.15)^2$$

$$\ln P_{\text{eq}} = -17.56832 \ln T + 0.0152556T - 9467.4/T + 133.67166$$

$$\Delta H_v = 66.47 \cdot 10^3(1 - T/T_c)^{0.3} \exp(-0.3T/T_c)$$

Helium

$$M = 4.0026 \cdot 10^{-3} \text{ kg mol}^{-1}$$

$$\sigma = 2.551 \cdot 10^{-10} \text{ m}$$

$$\varepsilon/k = 10.22 \text{ K}$$

$$\lambda_g = -2.45108 \cdot 10^{-2} + 1.12460 \cdot 10^{-3}T - 2.93123 \cdot 10^{-6}T^2 + 4.49646 \cdot 10^{-9}T^3 - 2.51948 \cdot 10^{-12}T^4$$

$$\eta_g = 1.4083 \cdot 10^{-6}T^{1.5}/(T + 70.22)$$

n-Nonane (v)–Helium (g)

$$D_{vg} = 1.11618 \cdot 10^{-5}RT^{1.76}/P_t$$

$$1/\alpha_{vg} = (-0.8238 - T/(23.06 - 0.2840T))(x_v + 0.1088) + 0.08962$$

$$\lambda_{vg} = x_v \lambda_v/(x_v + A_{vg}x_g) + x_v \lambda_v/(x_g + A_{gv}x_v)$$

SYMBOLS

A_{gv}, A_{vg}	parameters of dependence of mixture thermal conductivity on composition
C_p	molar heat capacity, $\text{J mol}^{-1} \text{K}^{-1}$
D_{vg}	binary diffusion coefficient, $\text{m}^2 \text{s}^{-1}$
g	gravitational acceleration constant, m s^{-2}
h	distance between plates, m
ΔH_v	molar enthalpy of vaporization, J mol^{-1}
M	molar mass, kg mol^{-1}
N	molar flux density, $\text{mol m}^{-2} \text{s}^{-1}$
P	pressure, Pa
Q	heat flux density between plates, $\text{W m}^{-2} \text{s}^{-1}$
R	gas constant, $\text{J mol}^{-1} \text{K}^{-1}$
s	parameter of temperature dependence of diffusion coefficient

T	temperature, K
x	mole fraction
V	molar volume, $\text{m}^{-3} \text{mol}^{-1}$
z	axial coordinate in chamber, m
α_{vg}	thermal diffusion factor, l
γ	surface tension, mN m^{-1}
ε/k	force constant for Lennard-Jones (6 – 12) potential, K
η	viscosity, Pa s
λ	thermal conductivity, $\text{W m}^{-1} \text{K}^{-1}$
ρ	density, kg m^{-3}
σ	force constant for Lennard-Jones (6 – 12) potential, m
ω	Pitzer acentric factor

Subscripts

l	liquid pool surface
2	surface of liquid on top plate
b	normal boiling point
c	critical state
eq	equilibrium value
g	gas
l	liquid
v	vapor

REFERENCES

1. Springer G. S.: *Adv. Heat Transfer* 14, 281 (1978).
2. Hodgson A. W.: *Adv. Colloid Interface Sci.* 21, 303 (1984).
3. Katz J. L.: *J. Chem. Phys.* 52, 4733 (1970).
4. Hung C.-H., Krasnopoler M. J., Katz J. L.: *J. Chem. Phys.* 90, 1856 (1989).
5. Adams J. W., Schmitt J. L., Zalabsky R. A.: *J. Chem. Phys.* 81, 5074 (1984).
6. Wagner P. E., Strey R. A.: *J. Chem. Phys.* 80, 5266 (1984).
7. Katz J. L.: *J. Stat. Phys.* 2, 137 (1970).
8. Dillmann A., Meier G. E. A.: *J. Chem. Phys.* 94, 3872 (1991).
9. Girshick S. L., Chiu C.-P.: *J. Chem. Phys.* 93, 1273 (1990).
10. Viisanen Y., Strey R. in: *Report Series in Aerosol Science*, No. 17 (M. Kulmala and K. Hameri, Eds), p. 82. Finnish Association for Aerosol Research, Helsinki 1991.
11. Smolik J., Vasakova J.: *Aerosol Sci. Technol.* 14, 406 (1991).
12. Katz J. L., Ostermier B. J.: *J. Chem. Phys.* 47, 478 (1967).
13. Smolik J., Vitovec J.: *Collect. Czech. Chem. Commun.* 41, 1471 (1976).
14. Smolik J., Vitovec J.: *Int. J. Heat Mass Transfer* 26, 975 (1982).
15. Katz J. L.: Unpublished results.
16. Katz J. L., Hung C.-H., Krasnopoler M. J. in: *Lecture Notes in Physics*, 309 (P. E. Wagner and G. Vali, Eds), p. 356. Springer, Berlin, Heidelberg 1988.
17. Reid R. C., Prausnitz J. M., Sherwood T. K.: *The Properties of Gases and Liquids*, 3rd ed. McGraw-Hill, New York 1977.
18. Tsouopoulos C.: *AIChE J.* 20, 263 (1974).

19. Hirschfelder J. O., Curtiss C. F., Bird R. B.: *Molecular Theory of Gases and Liquids*. Wiley, New York 1954.
20. Majer V., Svoboda V., Pechacek J., Hala S.: *J. Chem. Thermodyn.* *16*, 567 (1984).
21. Kokugan T., Shimizu M.: *J. Chem. Eng. Jpn.* *14*, 7 (1981).

Translation revised by J. Linek.